Short-Term Frequency Regulation and Inertia Emulation Using an MMC-Based MTDC System

Andres E. Leon, *Senior Member, IEEE*

***Abstract*—The continuous displacement of conventional power plants by converter-interfaced generation systems reduces the system inertia and may lead to a degradation of the frequency stability. A supplementary control strategy for multi-terminal dc (MTDC) systems to improve the frequency regulation is presented in this paper. The scenario where the MTDC system cannot resort to the power reserves of either other ac systems or offshore wind farms is particularly studied. The proposed control is able to independently support both the primary frequency regulation and the system inertia by using the capacitive energy of the MTDC grid converters. On the other hand, the reactive power of the converter stations is coordinately controlled to improve the damping of low-frequency electromechanical oscillations. The simultaneous frequency support of the MTDC system and onshore wind farms is also studied and validated in a practical multi-machine power system. Transient and small-signal stability analyses are performed to evaluate and quantify the improvements and the control limitations of the proposed scheme. This enhanced frequency control can increase the system reliability and reduce the required amount of spinning reserve, diminishing the operation costs and allowing to increase the penetration of renewable energy sources.**

***Index Terms*—Capacitive energy storage, distributed frequency control, inertia mimicry capability, multi-terminal high-voltage direct current (HVDC) systems, wind power integration.**

I. Introduction

MULTI-TERMINAL high-voltage direct current (HVDC) systems based on voltage-source converters (VSCs) of thousands of megawatts are now more feasible due to the development of the modular multilevel converter (MMC) technology [1]. These multi-terminal dc (MTDC) systems are a cost-effective and promising solution to integrate several distributed offshore wind farms (e.g., the North Sea grid), to build hybrid HVDC-AC systems (e.g., the European Supergrid project), and to interconnect multiple asynchronous ac systems [2]. On the other hand, the increasing participation of both renewable energy sources and dc interconnections in the power generation share reduces the total system inertia and leads to a degradation of the frequency stability [3]. This tendency poses a challenge for the control and operation of the system, requiring an increase of the spinning reserve and limiting the connection of converter-interfaced generation systems [4]–[6].

Several control strategies have been proposed to solve the lack of inertia of these electronically-interfaced systems and to provide frequency support without requiring additional energy storage devices. They make use of the kinetic energy stored in the rotating mass of wind turbines [7], the electrostatic energy stored in the converter capacitors [8]–[11], or a combination of both [12]–[15]. With this aim, the concepts of virtual synchronous machine, power-synchronization control and synchronverters have been studied to emulate the behavior of a conventional synchronous generator with a VSC [16]–[20].

MTDC systems can play an important role to improve the performance and reliability of the frequency regulation. The approaches to support the frequency control using these systems can be classified into two cases. In the first one, a supplementary control allows to share power reserves among asynchronous ac systems connected through an MTDC grid. In this way, independent ac systems can provide frequency support to another ac system after a frequency disturbance (see [21]–[24]). In the second case, a control strategy is designed so that offshore wind farms integrated with an MTDC system can receive the onshore frequency information and contribute to the frequency support of the land ac grid (see [25] and [26]). A control strategy combining these two cases is proposed in [27] and [28].

The present work focuses on a scenario not enclosed in the above cases. It considers a case where the MTDC grid is embedded in a single ac system (i.e., there is only one host ac grid), and there is no significant, or even null, amount of offshore generation. Consequently, the power reserve (energy) cannot be taken from either other asynchronous ac systems or offshore wind turbines. In this scenario, apart from the kinetic energy of wind turbines directly connected to the ac grid, the energy stored in the dc capacitors of the MTDC grid converters can be used to transiently support the system frequency. This is achieved by varying, within an acceptable range, the voltage level of the converter capacitors and exchanging their energy with the ac system [11].

The use of the energy stored in the converter stations is becoming more feasible with the MMC technology because this converter presents a capacitive energy storage capability higher than the one of the traditional two-level VSC [29]. Moreover, when considering the energy stored in all the MMC stations of an MTDC system, the frequency support is more significant. In

Manuscript received February 27, 2017; revised June 23, 2017 and August 15, 2017; accepted September 23, 2017. Date of publication September 27, 2017; date of current version April 17, 2018. This work was supported in part by the Consejo Nacional de Investigaciones Científicas y Técnicas and in part by the Universidad Nacional del Sur. Paper no. TPWRS-00287-2017.

The author is with the Instituto de Investigaciones en Ingeniería Eléctrica "Alfredo Desages", Universidad Nacional del Sur-Consejo Nacional de Investigaciones Científicas y Técnicas, Bahía Blanca 8000, Argentina (e-mail: aleon@iiie-conicet.gob.ar).

Color versions of one or more of the figures in this paper are available online at http://ieeexplore.ieee.org.

Digital Object Identifier 10.1109/TPWRS.2017.2757258

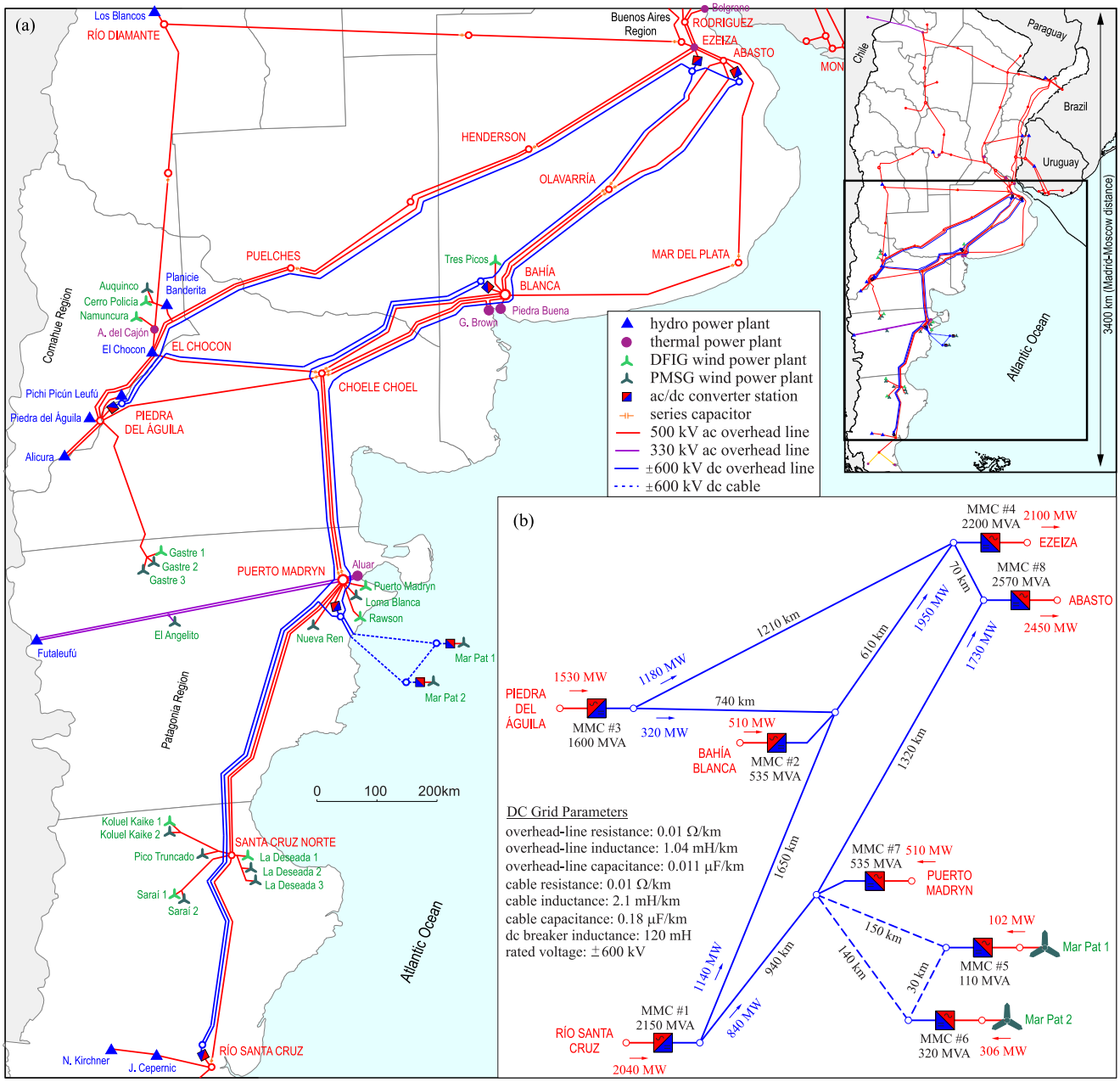

Fig. 1. Case study based on the Argentinian power system. (a) Geographical and single-line diagram. (b) Power flow and topology of the MTDC system.

the near future, networks might also combine the frequency support of various energy sources, such as wind farms and MTDC systems [9]. In this way, the control efforts are better distributed, and they do not depend only on wind turbines, which can suffer from stall, mechanical stress, and deloaded operation when performing this ancillary service [10]–[13]. The frequency support can also be provided at different time scales by complementing sources that can rapidly exchange energy with those that are slower but have a higher energy storage.

The schemes [8]–[11] consider a single supplementary control loop when using the capacitor energy to support the system frequency; therefore, they are not able to independently support both the primary frequency regulation and the system inertia. A higher control flexibility is obtained in [12]–[15] by adding the kinetic energy stored in offshore wind turbines. On the other hand, in the previous works, the converter capacitors are modeled as a concentrated capacitor on the dc side (i.e., traditional VSC topology); consequently, the dc grid voltage varies when the capacitor energy is released or absorbed during the frequency support. A different approach is used in the present work, where the frequency support is achieved by using the energy stored in the submodule capacitors of the MMCs. This varies the converter internal voltage, whereas the dc grid voltage is not affected.

The contributions of this work can be summarized as follows: (1) a control strategy that enables an independent provision of both short-term primary frequency regulation and virtual (or synthetic) inertia is proposed, allowing a more flexible control of

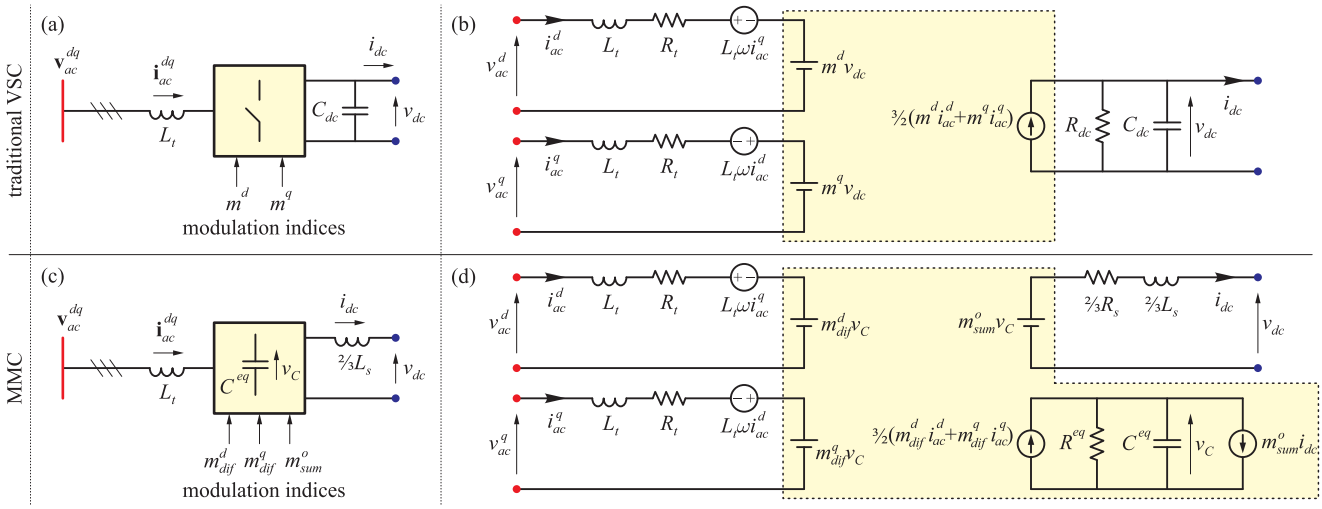

Fig. 2. Models of the ac/dc converter stations. (a) and (b): Configuration and equivalent electrical circuit of the traditional VSC. (c) and (d): Configuration and equivalent electrical circuit of the MMC.

the MTDC system to meet the frequency support requirements; (2) the simultaneous control of an MTDC grid and onshore wind farms to support the system frequency is analyzed and validated in a practical multi-machine power system; and (3) a centralized control is designed to coordinate the reactive power injected by the converter stations to damp low-frequency oscillations. In this way, both the active and the reactive power control loops are used to enhance the power system stability.

II. Case Study

The Argentinian transmission system operator (TSO) is planning to build a 2300-km long dc transmission line to connect the hydro power resources in the south of the country with the main load centers located in the Buenos Aires region (see Fig. 1). In addition, the expansion of the corridors in the Patagonia and Comahue regions is being studied to accommodate the large amounts of wind power generation projected there [30]. For these cases, the dc transmission is the most cost-effective solution due to the long distances involved. In this work, the planned dc lines are connected to create an MTDC grid, increasing the system reliability and improving the power flow control.

The considered electrical network is based on a future scenario of the Argentinian power system, and consists of an ac system with 272 buses, 77 power plants (55 synchronous generators and 22 wind farms), and an embedded eight-terminal dc grid able to transport 4.5 GW from remote renewable energy sources to the main load centers. The equivalent inertia constant of the system is $H_{sys} = 4.57$ s (on the system base $S_{sys} = 36.7$ GVA). The total load of the system is 28.8 GW, and the penetration level of onshore and offshore wind powers is 14% and 1.5%, respectively. A single-line diagram of the studied power system is shown in Fig. 1.

A. AC System Modeling

Synchronous generators are represented by the fourth-order two-axis model equipped with automatic voltage regulator (IEEE-ST1A), power system stabilizer (IEEE-PSS1A), and the corresponding (hydro or thermal) turbine-governor system [31]. The parameters of both the generators and the electrical network are taken from the reference guide of the Argentinian TSO.

Onshore wind farms are represented by aggregated models including the electric machine (permanent-magnet synchronous generator or doubly-fed induction generator), the wind turbine power curve, the power converters, the collector and transformer impedances, and the mechanical system represented by a two-mass model [32]. They also include the maximum power point tracking, the ac voltage regulator, and a supplementary control to provide frequency support. This supplementary control resorts to the kinetic energy stored in the rotating mass of the wind turbine to perform a short-term frequency regulation and to emulate inertia (no reserve power is required). An overload of 10% is temporarily allowed, and a washout filter is used to avoid steady-state contribution (see further details in [7] and [33]).

On the other hand, because the offshore wind farms do not participate in the studied frequency support, they are modeled as power sources delivering a constant power to the MTDC system [6].

B. DC System Modeling

Figure 2 shows the input-output model of both the traditional VSC and the MMC (see details of the MMC model in [34] and [35]). They have a similar representation on the ac side, but a different one on the dc side. The traditional VSC configuration is able to directly control the dc voltage v_{dc} due to the concentrated dc capacitor C_{dc}, thus, it has a voltage-source characteristic on the dc side (capacitive ending). On the other hand, the MMC directly controls the dc current i_{dc} through the inductance $2/3L_s$, having a current-source characteristic on the dc side (inductive ending) [36].

Because the submodule capacitors of the MMC are not directly coupled to the dc bus, the traditional VSC model does not reflect the operating characteristics of the MMC. The dc-side behavior of the MMC is better represented by modeling

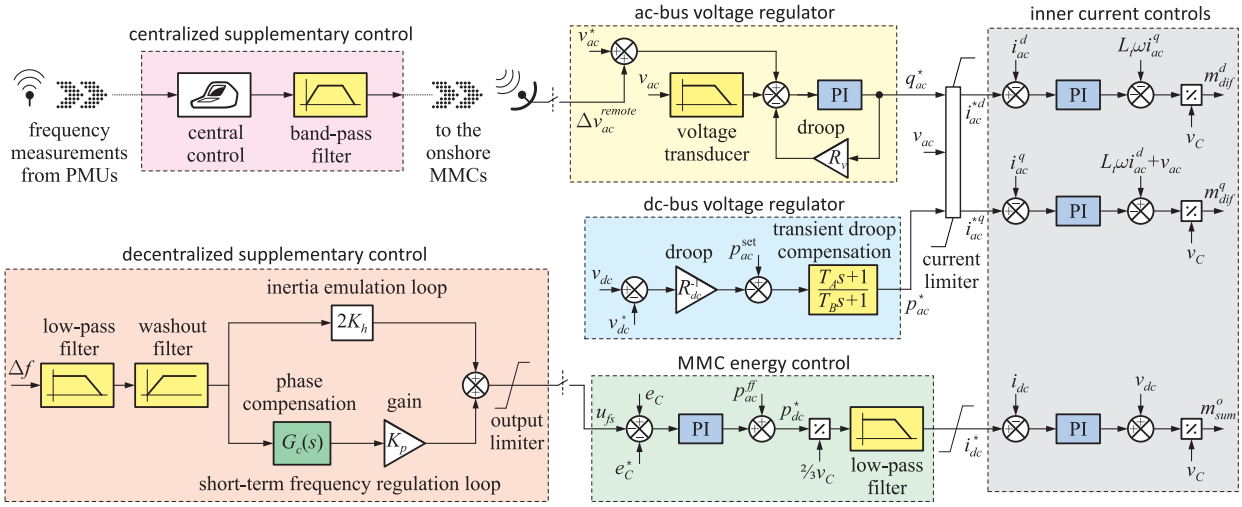

Fig. 3. Control strategy of the onshore MMC stations including both the supplementary and the standard controls.

the total converter voltage v_C (i.e., sum of all submodule capacitor voltages) and the dc-bus voltage v_{dc} as independent state variables [35]. In this work, the MMC model in Fig. 2(d) and the control strategy in Fig. 3 are used to represent the ac/dc converter stations. The per-unit converter parameters are taken from [1] with a stored energy of 35 kJ/MVA.

In the MTDC system, the stations #1, #3, and #8 control their active and reactive powers at constant set-points (i.e., they operate in *P-Q* mode), the stations #2, #4, and #7 share the dc grid voltage regulation using droop control (v_{dc}-*Q* mode), and the stations #5 and #6 extract the power generated by the offshore wind farms. In Fig. 3, the dc-bus voltage regulator has a droop of $R_{dc} = 5\%$ and a lead-lag block with constants $T_A = 0.025$ s and $T_B = 0.25$ s to transiently reduce the control gain, which avoids exciting resonance modes of the dc lines, as recommended by [37]. The droop of the ac-bus voltage regulator is set to $R_v = 5\%$, whereas an active power priority is considered in the current limiting scheme [38].

The transmission lines of the dc grid are represented by multiple π-sections (each of them smaller than 200 km) and include the dc breaker inductance at their terminals [39]. The power flow, dc grid parameters, and rated power of the converter stations are given in Fig. 1(b).

III. Supplementary Control Strategy for MMCs

The proposed supplementary control strategy is divided into two blocks: the first one is a decentralized control able to support the primary frequency regulation and the system inertia, and the second one is a centralized control designed to improve the damping of low-frequency electromechanical oscillations. The first control is based on local measurements and guarantees the frequency support even if remote communication is unavailable.

A. Decentralized Control

The frequency dynamics of a power system can be approximately described in per-unit values by

$$2H\Delta\dot{f} + D\Delta f = p_G - p_L + p_S \tag{1}$$

where Δf is the frequency deviation, the parameters H and D stand for the inertia and damping of the system, and p_G and p_L are the total generated and consumed powers, respectively. The term p_S represents a supplementary power that can be transiently released or absorbed by converter-based systems, such as variable-speed wind turbines and MTDC systems, to support the short-term primary frequency regulation and to emulate inertia. To perform these tasks, the supplementary power has two terms: one is proportional to the frequency deviation, and the other is proportional to the time derivative of the frequency, as follows

$$p_S = -K_p\Delta f - 2K_h\Delta\dot{f}. \tag{2}$$

Then, substituting (2) in (1) results in

$$2\left(H + K_h\right)\Delta\dot{f} + \left(D + K_p\right)\Delta f = p_G - p_L. \tag{3}$$

From (3), it is seen that the inertia and damping characteristics of the frequency dynamics can be modified by using the parameters K_h and K_p, respectively. In [7], these actions were performed by using the kinetic energy stored in the rotating mass of variable-speed wind turbines. However, in the case of using the electrostatic energy stored in the capacitors of the MMC, some modifications are required.

In an MMC, the dynamics of the total converter voltage is governed by the power balance between the ac and dc sides, as follows

$$\frac{C_{eq}}{S_B}\dot{v}_C = \frac{p_{ac} - p_{dc}}{v_C} \tag{4}$$

where C_{eq} is an equivalent capacitor, S_B is the rated power of the MMC, and the energy per volt-ampere is given by $e_C = \frac{1}{2}C_{eq}v_C^2/S_B$. Multiplying both sides of (4) by v_C yields

$$\dot{e}_C = p_{ac} - p_{dc} \tag{5}$$

where the power difference $\Delta p_C = p_{ac} - p_{dc}$ can be used to partially charge or discharge the capacitor C_{eq} and to provide the desired frequency support. Because the capacitor energy is controlled to perform this supplementary action, the phase shift

due to the dynamics (or transfer function) between the stored energy e_C and the power exchanged with the grid has to be compensated, as described below.

Applying the Laplace transform to the time-domain equations (2) and (5) gives

$$P_S(s) = -K_p \Delta F(s) - 2K_h s \Delta F(s) \tag{6}$$

$$sE_C(s) = \Delta P_C(s). \tag{7}$$

From (6) and (7), and considering that the power Δp_C works as the supplementary power p_S, the following equation is obtained

$$E_C(s) = -\frac{1}{s} K_p \Delta F(s) - 2K_h \Delta F(s). \tag{8}$$

As mentioned above, when the supplementary power is directly controlled, there are two terms: the first one, proportional to the frequency deviation, performs the short-term frequency regulation, and the second one, proportional to the time derivative of the frequency, performs the inertia emulation. On the other hand, when the energy e_C of the MMC is controlled to support the system frequency, equation (8) shows that the term proportional to the frequency deviation achieves the inertia emulation [i.e., the K_h term in (3)], and the term proportional to the integral of the frequency deviation achieves the short-term frequency regulation [i.e., the K_p term in (3)].

Consequently, to increase the system inertia using the MMC energy control, a signal proportional to the frequency deviation is added to the energy reference $e_C^\star$ (see Fig. 3). On the other hand, a phase compensation of the integral type (i.e., s^{-1}) is required to support the short-term frequency regulation. In the controller, this phase compensation is implemented using an imperfect integrator, such as

$$G_c(s) = \frac{1}{s+\varepsilon}. \tag{9}$$

The time constant ε is chosen small enough so that the compensator behaves as an integrator in the frequency range of interest, and to eliminate any potential steady-state offset in the compensator input ($\varepsilon = 0.15$ rad/s is considered in the study). Low-pass and washout filters with time constants of 40 ms and 8 s, respectively, are included to avoid both the interaction with high-frequency modes and the action of the supplementary control in the steady state (see the 'decentralized supplementary control' block in Fig. 3). To limit the submodule voltage variations and to keep the converter within a secure modulation range, the supplementary control signal is limited to prevent voltage variations beyond 15% (depending on the converter modulation limits, this value may be reduced to 10%). The choice of the parameters K_h and K_p is a trade-off between the allowed voltage variation and the amount of frequency support. Guidelines for the design of these parameters are given in the following subsection.

B. Design Guidelines for the Decentralized Control

The dynamics of the converter voltage can be rewritten from (4) as follows

$$\frac{C_{eq}}{S_B} v_C \dot{v}_C = \Delta p_A \tag{10}$$

where C_{eq} [F] is the equivalent capacitance, v_C [V] is the total converter voltage, Δp_A [pu] is the power released or absorbed by the equivalent capacitor, and S_B [VA] is the rated power of the MMC. To establish a link between the inertia time constant of conventional synchronous generators and the converter parameters, an analogous dynamics of a rotating mass is written as follows

$$\frac{2H_C}{f_s} \dot{f} = \Delta p_A \tag{11}$$

where H_C [s] is the inertia time constant, Δp_A [pu] is the power released or absorbed by the generator inertia, and f_s [Hz] is the nominal system frequency (50 Hz).

By equaling (10) and (11), and then integrating both sides with respect to time yields

$$\frac{2H_C}{f_s}(f_1 - f_0) = \frac{1}{2}\frac{C_{eq}}{S_B}\left(v_{C1}^2 - v_{C0}^2\right). \tag{12}$$

From (12), and after some mathematical manipulations, the inertia time constant emulated by the converter gives (see further details in [5] and [10])

$$H_C = \frac{\tau_C \left(\left(\frac{\Delta v_C}{v_{C0}} + 1 \right)^2 - 1 \right)}{\frac{2\Delta f}{f_s}} \tag{13}$$

where $\tau_C = \frac{1}{2} C_{eq} v_C^2 / S_B$ is the capacitor time constant. For an MMC with a submodule capacitance C^{SM}, and N submodules per arm, the equivalent capacitance is calculated as $C_{eq} = 6C^{\mathrm{SM}}/N$ [1]. The expression (13) relates the emulated inertia with both the converter voltage variation and the capacitive energy per volt-ampere for a given frequency deviation, and it can be used to evaluate the inertia emulation capability. For example, considering $\Delta v_C / v_{C0} = 15\%$, $\tau_C = 0.035$ s, and the maximum frequency deviation of the case study, the emulated inertia H_C is about 0.8 s (on the converter base). Then, by adding the contributions from the six onshore MMCs, the total emulated inertia is $\sum_{i=1\text{-}4,7,8} H_C S_{Bi} / S_{sys} = 0.2$ s (on the system base), representing an increase of 5% in the system inertia, which agrees with the simulation results obtained in Section IV.

The control parameter K_h plays the role of the emulated inertia time constant [see (3)]; therefore, the expression (13) can be used to assign an initial value to K_h. On the other hand, the control parameter K_p is equivalent to the droop constant of speed governors, which is typically in the order of 5%. In the case study, a good balance is found by choosing $K_h = 0.9$ s and $K_p^{-1} = 6\%$.

C. Centralized Controller

In order to use all the converter control flexibility, a centralized control is designed to improve the damping of low-

frequency oscillations by coordinately regulating the reactive power of the MMCs. Firstly, the centralized control receives the frequency measurements from phasor measurement units (PMUs) located in the onshore converter stations (i.e., the MMCs #1-#4, #7, and #8). Using this information, the set-points $v_{ac}^{\star}$ of the ac voltage regulators in these MMCs are transiently modified by adding a remote signal Δv_{ac}^{remote} (see Fig. 3). A communication delay of 200 ms is considered, and a band-pass filter is included to limit the control actions within the frequency range of interest (i.e., low-frequency inter-area modes in the range of 0.1 to 1.0 Hz). The procedure to design the centralized control is summarized as follows: (1) a reduced-order model of the system is firstly obtained using the balanced truncation method [40] and then, it is extended with a time-delay model to consider typical delays in communication channels; (2) a state-feedback control law is calculated based on an optimal quadratic technique [41]; and (3) the reduced-model states required in the control law implementation are estimated using a state observer. A detailed description of this centralized control approach can be found in [42] and [43].

Figure 3 shows a schematic block diagram of the complete control system.

IV. Transient Stability Analysis

Several non-linear time-domain simulations are performed to evaluate the transient response of the power system and the different supplementary controls. After a disturbance, the primary frequency regulation support can be quantified by the improvement in the frequency nadir, whereas the inertia emulation capability can be measured using the rate of change of frequency (RoCoF) [26]. In the following, when the system frequency deviations are compared, the average value of all the synchronous generator frequencies is considered.

The ability of the decentralized control to independently support both the primary frequency regulation and the inertial response is shown in Fig. 4, where a 400-MW load step is applied at the bus OLAVARRÍA (see Fig. 1). In this test, the frequency support is provided by both the MMCs and the onshore wind farms, and the centralized control is turned off. First, only the primary frequency regulation is supported (see the first column in Fig. 4), showing an improvement of 18% in the frequency nadir, no significant modification in the maximum deviation of the RoCoF (i.e., no inertia emulation), and a discharge of 10.5% in the converter voltage. Second, only the inertia emulation is performed (second column in Fig. 4); in this case, the maximum RoCoF is reduced by 7%. Third, both the primary frequency regulation and the inertia are supported (third column); in this scenario, the frequency nadir and the RoCoF are improved by 20% and 7.5%, respectively, whereas the voltage varies 15%.

The impact of both the centralized control and the simultaneous use of MMCs and wind farms on the frequency support is shown in Fig. 5. Three cases are analyzed having the short-term frequency regulation and the inertia emulation control loops active. In the first case, the frequency support is provided only by the MMCs using decentralized controls; the second case adds the centralized control to the MMCs, and the third case completes the control strategy by supporting the system frequency with both the MMCs and the onshore wind farms. Although some improvement in the frequency nadir is seen when considering Fig. 5(a1) and (a2), because the centralized control is designed to damp inter-area electromechanical oscillations, the addition of this control does not significantly improve the frequency response (compare the first column to the second col-

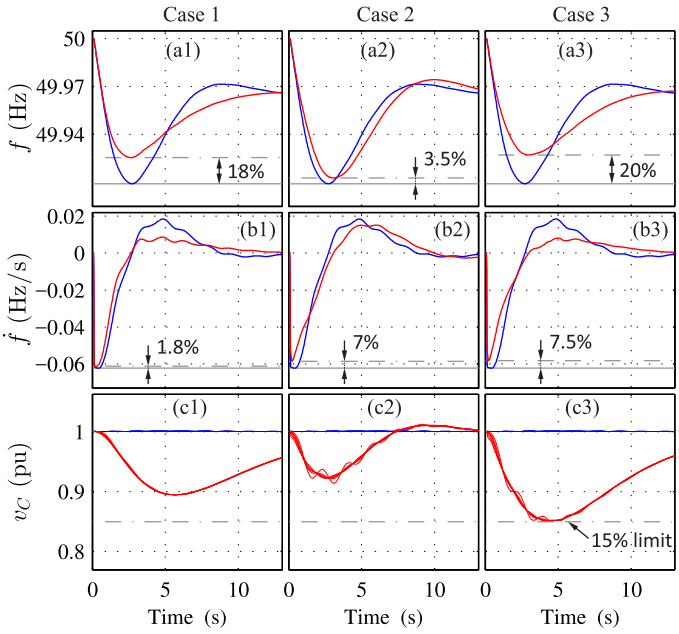

Fig. 4. Transient response to a 400-MW load step with and without the supplementary controls (red and blue lines, respectively). Case 1: short-term primary frequency regulation. Case 2: inertia emulation. Case 3: both short-term primary frequency regulation and inertia emulation.

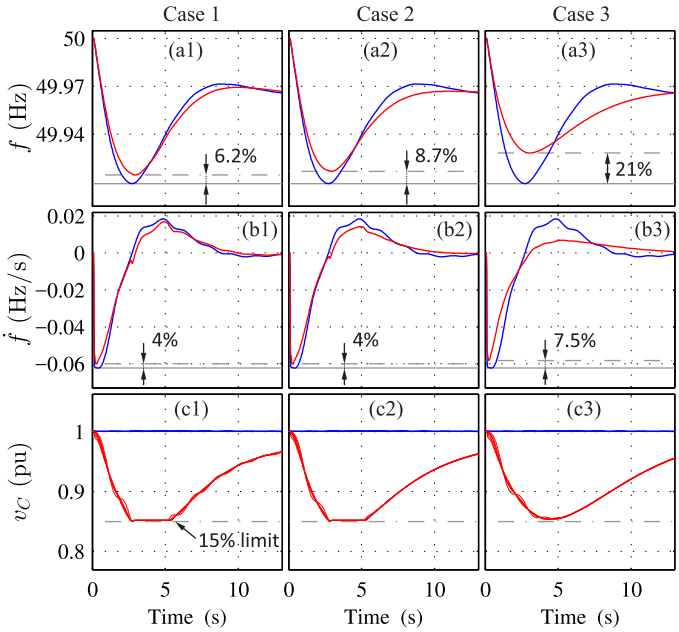

Fig. 5. Transient response to a 400-MW load step with and without the supplementary controls (red and blue lines, respectively). Case 1: decentralized controls in the MMCs. Case 2: decentralized and centralized controls in the MMCs. Case 3: supplementary controls in both the MMCs and the onshore wind farms.

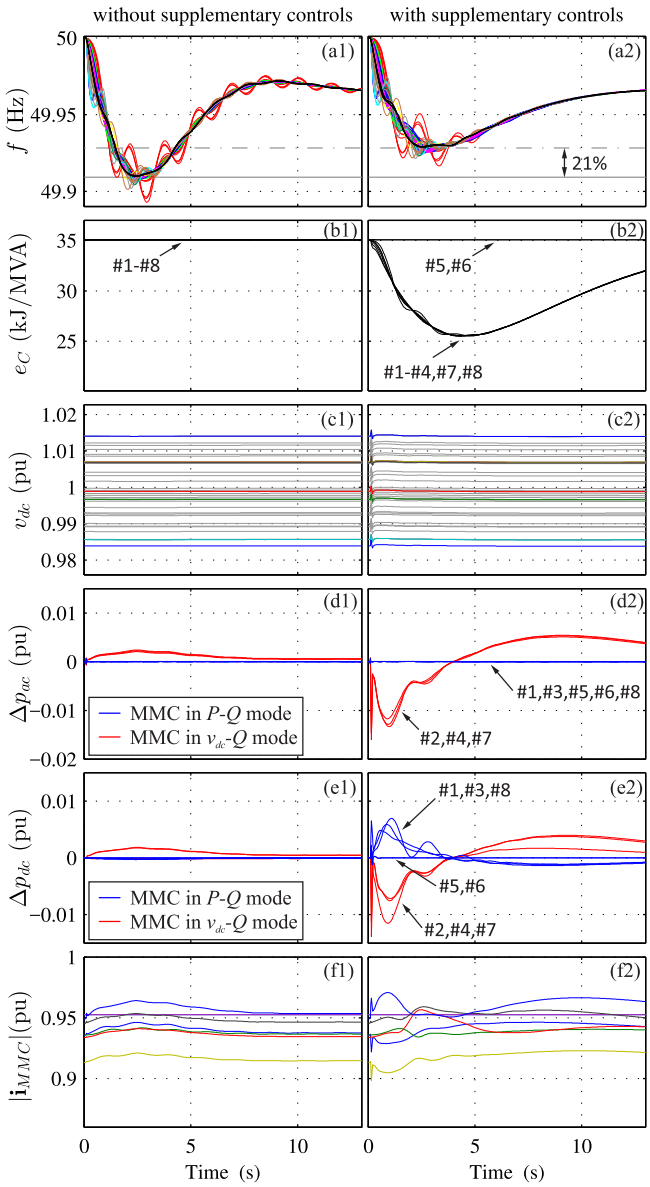

Fig. 6. Transient response to a 400-MW load step without and with the supplementary controls (first and second columns, respectively). (a) Frequency of the synchronous generators. (b) Total converter energy. (c) DC grid voltages. (d) AC-side power variation of the converters. (e) DC-side power variation of the converters. (f) Magnitude of the converter ac currents.

umn in Fig. 5). On the other hand, improvements of 21% in the frequency nadir and 7.5% in the RoCoF are achieved by implementing the complete supplementary control strategy and by using both the MMCs and the wind farms (compare blue lines to red lines in the third column in Fig. 5). Fig. 5(c) shows the variation in the total converter voltage. Note that the inclusion of the wind farms in the frequency support alleviates the supplementary control effort of the MMCs sharing the control burden, which results in a lower voltage variation [compare Fig. 5(c2) to (c3)].

The previous load step is repeated to show the transient response of different states of the power system. The first and the second columns in Fig. 6 present the cases without supplementary controls and with all the supplementary controls active.

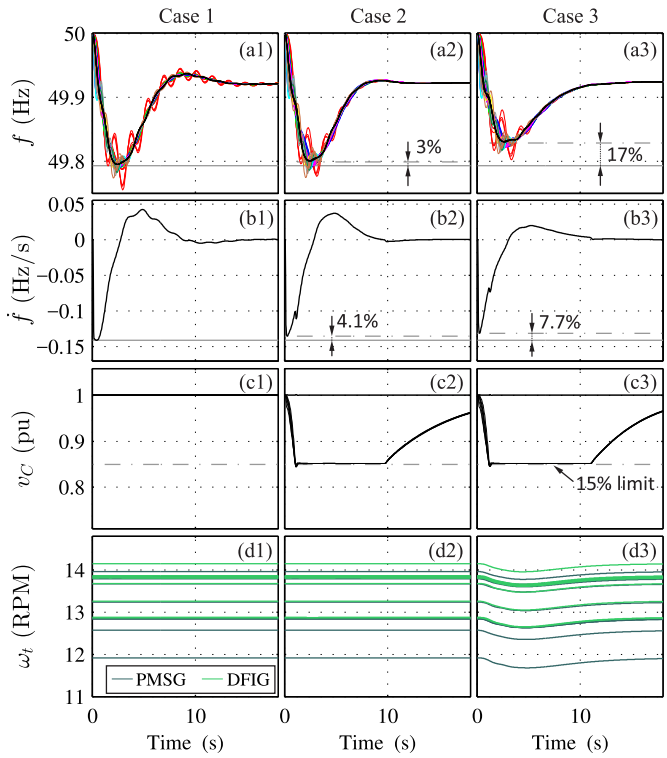

Fig. 7. Transient response to a 900-MW load step. Case 1: without supplementary frequency support. Case 2: with frequency support of the MMC stations. Case 3: with frequency support of both MMC stations and onshore wind farms.

In Fig. 6(a), the improvement of both the frequency nadir and the electromechanical oscillation damping is observed [compare Fig. 6(a1) to (a2)]. The energy variation of the MMCs is shown in Fig. 6(b). The studied frequency support does not use the offshore stations; therefore, their energies remain constant [see the MMCs #5 and #6 in Fig. 6(b2)]. The voltage of the dc grid is given in Fig. 6(c), where the colored lines represent the terminal nodes of the MTDC system, and the gray lines represent the intermediate nodes of the cascaded π-sections in the dc transmission lines. Because the submodule capacitor energies of the MMCs are used in the frequency support, only small transients are observed in the dc grid voltages, which remain almost constant during the frequency disturbance. The ac- and dc-side power variations of the eight converter stations are shown in Fig. 6(d) and (e), respectively. The MMCs #1, #3 and #8 (operating in *P*-*Q* mode) and the offshore MMCs #5 and #6 keep their ac power constant, whereas the MMCs #2, #4 and #7 (operating in v_{dc}-*Q* mode) perform the energy exchange with the ac grid [see Fig. 6(d2)]. The MMCs operating in *P*-*Q* mode inject the converter energy into the dc grid, and then this energy is delivered to the ac grid through the MMCs operating in v_{dc}-*Q* mode [see Fig. 6(e2)]. Figure 6(f2) shows that the converter ac currents remain within acceptable values during the disturbance.

A more severe test with a loss of infeed of 900 MW is presented in Fig. 7. This power imbalance is equivalent to the loss of the largest generating unit in the system and allows to analyze the supplementary control behavior when the maximum support capability is reached [see Fig. 7(c2) and (c3)]. By comparing

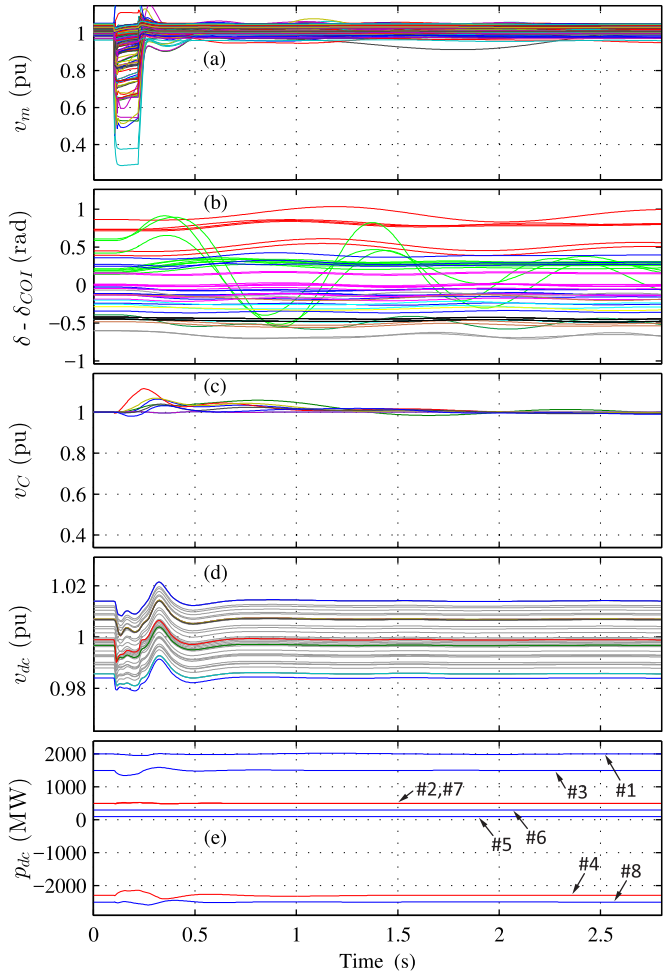

Fig. 8. Three-phase fault test. (a) AC bus voltages. (b) Load angle of the synchronous generators (each color represents a different region of the system). (c) Total converter voltages. (d) DC grid voltages. (e) DC-side power of the converters.

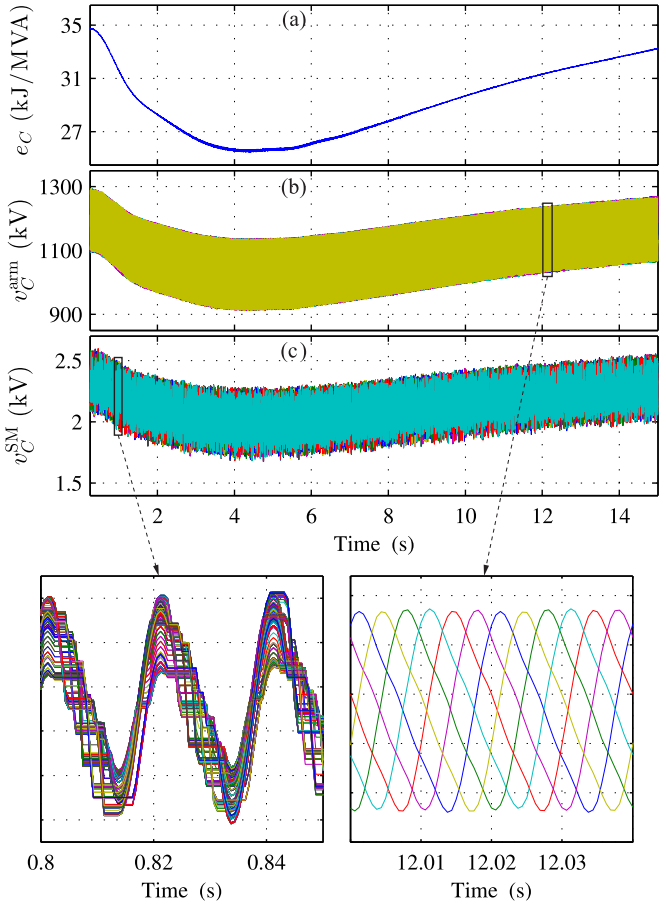

Fig. 9. Transient response to a 400-MW load step with the supplementary controls active. (a) Total stored energy of the MMC station #3. (b) Sum of all capacitor voltages in each arm. (c) Submodule capacitor voltages of the phase-a positive arm.

the three presented cases, it is observed that the onshore wind farms contribute to the primary frequency regulation support in a higher proportion than when it is only used the energy stored in the MTDC grid converters. This is especially the case for large frequency deviations, where the limited energy of the converter capacitors is more evident. However, in all the studied tests, similar improvements in the maximum RoCoF are observed when using either the MMCs or the wind farms. Therefore, the use of the energy stored in the MMC stations can complement the inertia support of wind turbines and reduce their mechanical stress (see [12] and [14]).

Finally, a 120-ms three-phase fault is applied at the bus A.CAJON (near the bus EL CHOCON) and cleared by opening the faulted line (all the supplementary controls are active). The transient response of the different variables shows that the system can properly ride-through the fault and reach a new equilibrium point after a transient period (see Fig. 8).

V. Verification on a Detailed MMC Model

In this section, the performance of the proposed supplementary control is verified on an MMC considering the dynamics of the individual submodule voltages. The converter model with information on the submodule level is obtained from [44], and the submodule capacitor voltages are controlled using the energy-based control scheme described in [45] and [46]. This control scheme consists of three blocks. In the first one (called intra-arm balancing), the capacitor voltages inside each arm are evenly distributed using the sorting method; in the second one, a control loop manages the circulating current to balance the arm energies (inter-arm balancing); and in the third one, the total converter energy is regulated by controlling the power flow between the ac and dc sides. The proposed supplementary control is added to the last control block, whereas the rest of the converter controls remain unchanged.

The test shown in Fig. 6 with all the supplementary control active is repeated here, considering a detailed representation of the MMC station #3. The converter is built with 512 submodules per arm and a submodule capacitance of 6.6 mF. Figure 9(a) shows how the MMC stored energy is transiently released to support the system frequency. The appropriate balance of the six arm voltages (i.e., inter-arm balancing) is observed in the zoom window of Fig. 9(b). Finally, Fig. 9(c) shows that the 512 submodule voltages of the phase-a positive arm uniformly reduce their average value as the MMC energy is released; then, they recover their nominal value after the frequency disturbance. This test

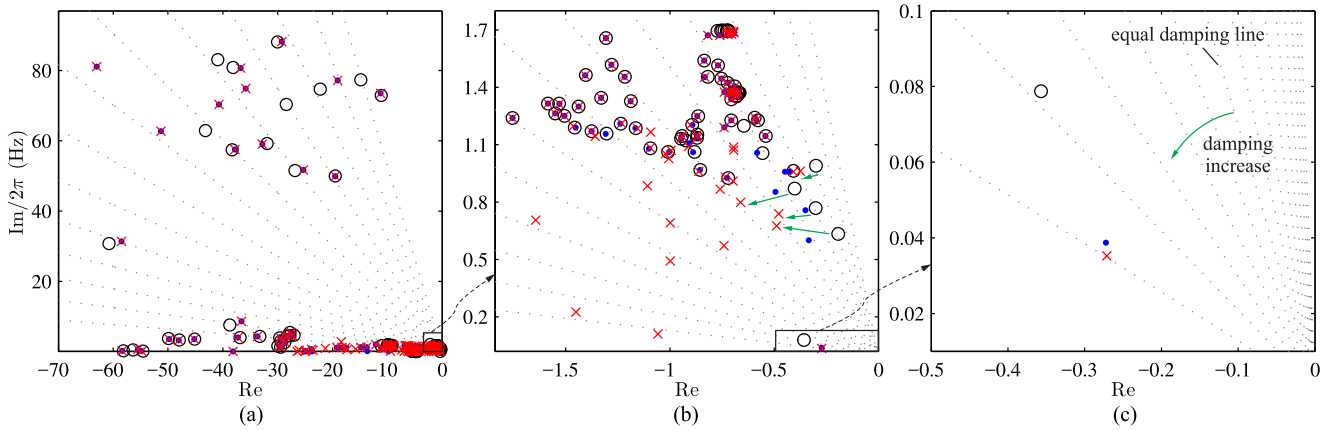

Fig. 10. Eigenvalues of the system with and without the supplementary controls. Comparison of the base system (black circle markers), the system with the decentralized supplementary control (blue dot markers), and the system with the decentralized and centralized supplementary controls (red cross markers).

shows that the internal controls of the MMC can balance the individual submodule voltages, leaving the free regulation of the total converter energy (for frequency support) to the supplementary control.

VI. Small-Signal Stability Analysis

In this section, the eigenvalues of the system are presented to evaluate the impact of the supplementary controls on the small-signal stability (dead-band blocks are not considered in this analysis [6]). Three cases are compared and shown in Fig. 10. The first one is the power system without supplementary controls (black circle markers); the second case considers the frequency support of the decentralized controls in MMCs and onshore wind farms (blue dot markers); and the third case includes both the decentralized and the centralized controls (red cross markers). The frequency range where the main resonance modes of the dc lines are located is shown in Fig. 10(a); the frequency range of the electromechanical modes is presented in Fig. 10(b); and Fig. 10(c) shows the eigenvalue associated with the governor systems and responsible for the frequency dynamics.

It can be seen that the decentralized control (second case) mainly improves the damping ratio of the governor (frequency) mode [compare the blue dot marker to the black circle marker in Fig. 10(c)]. On the other hand, the inclusion of the centralized control (third case) considerably improves the damping ratio of the electromechanical modes in the frequency range of the inter-area oscillations [see the green arrows and compare the red cross markers to the black circle markers in Fig. 10(b)]. Finally, Fig. 10(a) shows that no significant impact on the dc grid modes is evidenced by the inclusion of the supplementary controls. Therefore, the objectives of improving the frequency response and the inter-area oscillation damping are properly achieved from a small-signal point of view.

VII. Conclusion

The frequency support using both an MTDC system and onshore wind farms was investigated in this work. A case study was analyzed where the MTDC system cannot resort to the power reserves of either other ac systems or offshore wind farms to mitigate frequency deviations. A decentralized supplementary control was designed for MTDC grid converters to provide an independent support of both the primary frequency regulation and the system inertia. This improves the control flexibility of previous schemes that support the system frequency by managing the capacitor energy of the converter with only one supplementary control loop. In addition, a centralized control to coordinate the reactive power injected by the converter stations was included to damp low-frequency electromechanical oscillations. The proposed control strategy was validated and the improvements were quantified in a practical multi-machine HVDC-AC system performing transient and small-signal stability analyses. The obtained results show that the stability and reliability of the frequency control can be improved even when the power generation share of converter-interfaced generation systems increases. This kind of enhanced frequency control can reduce the required amount of spinning reserve, increase the penetration of renewable energies, and facilitate meeting the grid code requirements.

References

[1] J. Peralta, H. Saad, S. Dennetiere, J. Mahseredjian, and S. Nguefeu, "Detailed and averaged models for a 401-level MMC-HVDC system," *IEEE Trans. Power Del.*, vol. 27, no. 3, pp. 1501–1508, Jul. 2012.

[2] P. McNamara and F. Milano, "Model predictive control based AGC for multi-terminal HVDC-connected AC grids," *IEEE Trans. Power Syst.*, to be published.

[3] E. Rakhshani and P. Rodriguez, "Inertia emulation in AC/DC interconnected power systems using derivative technique considering frequency measurement effects," *IEEE Trans. Power Syst.*, vol. 32, no. 5, pp. 3338–3351, Sep. 2017.

[4] H. Silva-Saravia, H. Pulgar-Painemal, and J. M. Mauricio, "Flywheel energy storage model, control and location for improving stability: The Chilean case," *IEEE Trans. Power Syst.*, vol. 32, no. 4, pp. 3111–3119, Jul. 2017.

[5] M. Ashabani and Y. A. R. I. Mohamed, "Novel comprehensive control framework for incorporating VSCs to smart power grids using bidirectional synchronous-VSC," *IEEE Trans. Power Syst.*, vol. 29, no. 2, pp. 943–957, Mar. 2014.

[6] S. Akkari, J. Dai, M. Petit, and X. Guillaud, "Interaction between the voltage-droop and the frequency-droop control for MT-HVDC systems," *IET Gener., Transm. Distrib.*, vol. 10, no. 6, pp. 1345–1352, 2016.

[7] J. Mauricio, A. Marano, A. Gomez-Exposito, and J. Martinez Ramos, "Frequency regulation contribution through variable-speed wind energy conversion systems," *IEEE Trans. Power Syst.*, vol. 24, no. 1, pp. 173–180, Feb. 2009.

[8] C. E. Spallarossa, M. M. C. Merlin, and T. C. Green, "Augmented inertial response of multi-level converters using internal energy storage," in *Proc. IEEE Int. Energy Conf.*, Apr. 2016, pp. 1–6.
[9] O. D. Adeuyi *et al.*, "Frequency support from modular multilevel converter based multi-terminal HVDC schemes," in *Proc. IEEE PES General Meeting*, Jul. 2015.
[10] J. Zhu, C. D. Booth, G. P. Adam, A. J. Roscoe, and C. G. Bright, "Inertia emulation control strategy for VSC-HVDC transmission systems," *IEEE Trans. Power Syst.*, vol. 28, no. 2, pp. 1277–1287, May 2013.
[11] J. Zhu, J. M. Guerrero, W. Hung, C. D. Booth, and G. P. Adam, "Generic inertia emulation controller for multi-terminal voltage-source-converter high voltage direct current systems," *IET Renew. Power Gener.*, vol. 8, no. 7, pp. 740–748, Sep. 2014.
[12] A. Junyent-Ferre, Y. Pipelzadeh, and T. C. Green, "Blending HVDC-link energy storage and offshore wind turbine inertia for fast frequency response," *IEEE Trans. Sustain. Energy*, vol. 6, pp. 1059–1066, Jul. 2015.
[13] Y. Li, Z. Xu, and K. P. Wong, "Advanced control strategies of PMSG-based wind turbines for system inertia support," *IEEE Trans. Power Syst.*, vol. 32, no. 4, pp. 3027–3037, Jul. 2017.
[14] H. Liu and Z. Chen, "Contribution of VSC-HVDC to frequency regulation of power systems with offshore wind generation," *IEEE Trans. Energy Convers.*, vol. 30, no. 3, pp. 918–926, Sep. 2015.
[15] Y. Li, Z. Zhang, Y. Yang, Y. Li, H. Chen, and Z. Xu, "Coordinated control of wind farm and VSC-HVDC system using capacitor energy and kinetic energy to improve inertia level of power systems," *Int. J. Elect. Power Energy Syst.*, vol. 59, pp. 79–92, 2014.
[16] L. Zhang, L. Harnefors, and H. P. Nee, "Power-synchronization control of grid-connected voltage-source converters," *IEEE Trans. Power Syst.*, vol. 25, no. 2, pp. 809–820, May 2010.
[17] W. Zhang, A. M. Cantarellas, J. Rocabert, A. Luna, and P. Rodriguez, "Synchronous power controller with flexible droop characteristics for renewable power generation systems," *IEEE Trans. Sustain. Energy*, vol. 7, no. 4, pp. 1572–1582, Oct. 2016.
[18] E. Rakhshani, D. Remon, A. M. Cantarellas, J. M. Garcia, and P. Rodriguez, "Virtual synchronous power strategy for multiple HVDC interconnections of multi-area AGC power systems," *IEEE Trans. Power Syst.*, vol. 32, no. 3, pp. 1665–1677, May 2017.
[19] R. Aouini, B. Marinescu, K. B. Kilani, and M. Elleuch, "Synchronverter-based emulation and control of HVDC transmission," *IEEE Trans. Power Syst.*, vol. 31, no. 1, pp. 278–286, Jan. 2016.
[20] S. I. Nanou and S. A. Papathanassiou, "Grid code compatibility of VSC-HVDC connected offshore wind turbines employing power synchronization control," *IEEE Trans. Power Syst.*, vol. 31, no. 6, pp. 5042–5050, Nov. 2016.
[21] T. M. Haileselassie and K. Uhlen, "Primary frequency control of remote grids connected by multi-terminal HVDC," in Proc. IEEE *PES General Meeting*, Jul. 2010, pp. 1–6.
[22] J. Dai, Y. Phulpin, A. Sarlette, and D. Ernst, "Coordinated primary frequency control among non-synchronous systems connected by a multi-terminal high-voltage direct current grid," *IET Gener., Transm. Distrib.*, vol. 6, no. 2, pp. 99–108, Feb. 2012.
[23] N. R. Chaudhuri, R. Majumder, and B. Chaudhuri, "System frequency support through multi-terminal DC (MTDC) grids," *IEEE Trans. Power Syst.*, vol. 28, no. 1, pp. 347–356, Feb. 2013.
[24] M. Andreasson, R. Wiget, D. V. Dimarogonas, K. H. Johansson, and G. Andersson, "Distributed frequency control through MTDC transmission systems," *IEEE Trans. Power Syst.*, vol. 32, no. 1, pp. 250–260, Jan. 2017.
[25] B. Silva, C. L. Moreira, L. Seca, Y. Phulpin, and J. A. P. Lopes, "Provision of inertial and primary frequency control services using offshore multi-terminal HVDC networks," *IEEE Trans. Sustain. Energy*, vol. 3, no. 4, pp. 800–808, Oct. 2012.
[26] I. M. Sanz, B. Chaudhuri, and G. Strbac, "Inertial response from offshore wind farms connected through DC grids," *IEEE Trans. Power Syst.*, vol. 30, no. 3, pp. 1518–1527, May 2015.
[27] F. D. Bianchi and J. L. Domínguez-García, "Coordinated frequency control using MT-HVDC grids with wind power plants," *IEEE Trans. Sustain. Energy*, vol. 7, no. 1, pp. 213–220, Jan. 2016.
[28] O. D. Adeuyi, M. Cheah-Mane, J. Liang, and N. Jenkins, "Fast frequency response from offshore multi-terminal VSC-HVDC schemes," *IEEE Trans. Power Del.*, to be published.
[29] S. Rohner, S. Bernet, M. Hiller, and R. Sommer, "Modulation, losses, and semiconductor requirements of modular multilevel converters," *IEEE Trans. Ind. Electron.*, vol. 57, no. 8, pp. 2633–2642, Aug. 2010.
[30] A. E. Leon, "Integration of DFIG-based wind farms into series-compensated transmission systems," *IEEE Trans. Sustain. Energy*, vol. 7, no. 2, pp. 451–460, Apr. 2016.
[31] P. Kundur, *Power System Stability and Control*. New York, NY, USA: McGraw-Hill, 1994.
[32] O. Anaya-Lara, N. Jenkins, J. Ekanayake, P. Cartwright, and M. Hughes, *Wind Energy Generation: Modelling and Control*. New York, NY, USA: Wiley, 2009.
[33] J. Morren, S. De Haan, W. Kling, and J. Ferreira, "Wind turbines emulating inertia and supporting primary frequency control," *IEEE Trans. Power Syst.*, vol. 21, no. 1, pp. 433–434, Feb. 2006.
[34] D. Ludois and G. Venkataramanan, "Simplified terminal behavioral model for a modular multilevel converter," *IEEE Trans. Power Electron.*, vol. 29, no. 4, pp. 1622–1631, Apr. 2014.
[35] J. Freytes, L. Papangelis, H. Saad, P. Rault, T. V. Cutsem, and X. Guillaud, "On the modeling of MMC for use in large scale dynamic simulations," in *Proc. Power Syst. Comput. Conf.*, Jun. 2016, pp. 1–7.
[36] D. Soto-Sanchez and T. Green, "Control of a modular multilevel converter-based HVDC transmission system," in *Proc. Eur. Conf. Power Electron. Appl.,* Aug. 2011, pp. 1–10.
[37] C. Gavriluta, I. Candela, C. Citro, A. Luna, and P. Rodriguez, "Design considerations for primary control in multi-terminal VSC-HVDC grids," *Electr. Power Syst. Res.*, vol. 122, pp. 33–41, 2015.
[38] F. B. Ajaei and R. Iravani, "Dynamic interactions of the MMC-HVDC grid and its host AC system due to AC-side disturbances," *IEEE Trans. Power Del.*, vol. 31, no. 3, pp. 1289–1298, Jun. 2016.
[39] W. Wang, M. Barnes, O. Marjanovic, and O. Cwikowski, "Impact of DC breaker systems on multiterminal VSC-HVDC stability," *IEEE Trans. Power Del.*, vol. 31, no. 2, pp. 769–779, Apr. 2016.
[40] J. Sanchez-Gasca and J. Chow, "Power system reduction to simplify the design of damping controllers for interarea oscillations," *IEEE Trans. Power Syst.*, vol. 11, no. 3, pp. 1342–1349, Aug. 1996.
[41] A. E. Leon, J. M. Mauricio, A. Gomez-Exposito, and J. A. Solsona, "Hierarchical wide-area control of power systems including wind farms and FACTS for short-term frequency regulation," *IEEE Trans. Power Syst.*, vol. 27, no. 4, pp. 2084–2092, Nov. 2012.
[42] Y. Pipelzadeh, B. Chaudhuri, and T. Green, "Wide-area power oscillation damping control through HVDC: A case study on Australian equivalent system," in *Proc. IEEE Power Energy Soc. Meeting*, 2010, pp. 1–7.
[43] A. E. Leon and J. A. Solsona, "Power oscillation damping improvement by adding multiple wind farms to wide-area coordinating controls," *IEEE Trans. Power Syst.*, vol. 29, no. 3, pp. 1356–1364, May 2014.
[44] J. Wang, R. Burgos, and D. Boroyevich, "Switching-cycle state-space modeling and control of the modular multilevel converter," *IEEE J. Emerg. Sel. Topics Power Electron.*, vol. 2, no. 4, pp. 1159–1170, Dec. 2014.
[45] S. Cui, S. Kim, J.-J. Jung, and S.-K. Sul, "A comprehensive cell capacitor energy control strategy of a modular multilevel converter (MMC) without a stiff DC bus voltage source," in *Proc. Annu. IEEE Appl. Power Electron. Conf. Expo.,* Mar. 2014, pp. 602–609.
[46] A. E. Leon and S. J. Amodeo, "Energy balancing improvement of modular multilevel converters under unbalanced grid conditions," *IEEE Trans. Power Electron.*, vol. 32, no. 8, pp. 6628–6637, Aug. 2017.

Andres E. Leon (S'05–M'13–SM'16) received the degree in electrical engineering from the Universidad Nacional del Comahue, Neuquén, Argentina, and the Doctoral degree in control systems from the Universidad Nacional del Sur, Bahía Blanca, Argentina, in 2005 and 2011, respectively. Since 2012, he has been a Researcher in the National Scientific and Technical Research Council. He is currently working with the Research Institute of Electrical Engineering "Alfredo Desages", Bahía Blanca, Argentina. His research interests include power system control and wind energy conversion systems. He is an Associate Editor of the IEEE TRANSACTIONS ON SUSTAINABLE ENERGY.